Electric Power Systems Research 129 (2015) 160–169

Contents lists available at ScienceDirect

Electric Power Systems Research

journal homepage: www.elsevier.com/locate/epsr

Power system reliability evaluation considering cyber-malfunctions in substations

Hangtian Lei*, Chanan Singh

Department of Electrical and Computer Engineering, Texas A&M University, College Station, TX 77843, USA

ARTICLE INFO

Article history:
Received 22 April 2015
Received in revised form 3 August 2015
Accepted 5 August 2015
Available online 28 August 2015

Keywords:
Cyber-physical interface matrix
Hidden failure
Protection system
Reliability
Switching

ABSTRACT

Protection system failures have been recognized as major causes of expanded outages and thereby affect bulk power system reliability. With the rapid progress of smart grid technologies, legacy protection systems with hardwired architecture are being gradually replaced by computer and communication networks consisting of multi-functional and smart Intelligent Electronic Devices (IEDs). In this paper, a systematic methodology for considering the effect of cyber-malfunctions in substations on power system reliability is proposed by extending the concepts we previously presented. The Roy Billinton Test System (RBTS) is extended to include substation protection systems with modern architecture, which is an important step as a test system like this is currently unavailable. The proposed approach is then demonstrated on this test system. The quantitative relationship between switching time and system-wide energy unavailability is studied. The results of our study clearly indicate the impact of protection system failures on system-wide reliability indices and signify the importance of accelerating line switching process. Furthermore, the overall methodology used in this paper provides a tractable and scalable option for the reliability evaluation of large cyber-physical power systems.

1. Introduction

The quantitative reliability indices of bulk power systems are important to utility companies, vendors, and regulators for planning, operation, maintenance, and regulatory purposes. Studies of bulk power system reliability evaluation have been mostly focusing on the current-carrying part. The pertinent theories and methodologies are well established and documented [1–3].

In bulk power system reliability evaluation, protection systems are typically assumed to be perfectly reliable so that the failure of a current-carrying component will result in the isolation of that component only. This assumption may neglect the impact of protection system failures on system-wide reliability indices. It has been recognized that protection system hidden failures are common causes of multiple or cascading outages [4–7]. Some studies [6–10] have been done to consider protection system failures and the results show that protection system failure modes have significant effects on evaluated reliability indices.

A protection system consists of circuit breakers, current and voltage transformers, communication cables, protective relays, and possibly some auxiliary devices [11–13]. With the advent of microprocessor-based relays and the rapid progress of communication technologies, modern protection panels are equipped with multifunctional Intelligent Electronic Devices (IEDs) that are connected to communication networks [14–17].

In composite power system reliability evaluation, due to the variety of protection system architectures as well as the diversity of control and communication mechanisms, it is hard to explicitly model protection systems with detailed configurations. As a result, in most of the previous work, protection system failures were either concentrated on circuit breaker trip mechanisms [6] or represented abstractly by multistate models [7–10] without showing the technical details regarding protection system elements as well as their connections. Due to the absence of such details, the interdependencies between protection elements and power equipment were not covered in those publications. In [18,19], to study the direct and indirect cyber-physical interdependencies, some mathematical terms and operations were defined and proposed with applications on small test systems including monitoring, control, and protection features. The results in [18,19] provide valuable information that indicates the impact of cyber element failures on physical system reliability indices. However, excessive self-defined

* Corresponding author. Tel.: +1 979 571 0474.
E-mail addresses: hlei7@tamu.edu (H. Lei), singh@ece.tamu.edu (C. Singh).

http://dx.doi.org/10.1016/j.epsr.2015.08.010
0378-7796/

reliability terms and tedious mathematical operations were introduced in [18,19]. These terms are hardly available from engineering practice, making it difficult to implement the overall methodology in practical applications. Reference [20] proposed a more systematic and scalable methodology of performing the overall analysis in a tractable fashion with the use of *Cyber-Physical Interface Matrix* (*CPIM*). In [20], a typical substation protection system with detailed architecture was designed and analyzed as an example to illustrate the procedures of obtaining a CPIM. The steps on how to use a CPIM in composite power system reliability evaluation were also formulated.

The composite power system displayed in [20] is simple and is used for illustration only. The overall methodology with the use of CPIM needs to be further demonstrated with its implementation on a standard test system so that the impact of protection failures on system-wide reliability indices can be numerically validated. Also, the scalability of the overall methodology needs further illustration as this is very important to its application for large power systems. Moreover, the unavailability of standard reliability test systems containing practical protection features is an obstacle for validation of the impact of protection failures on system-wide reliability indices. The extension of the Roy Billinton Test System (RBTS) [21] performed in this paper provides valuable information for developing standard reliability test systems including protection features and will thereby benefit future studies in this area. With these objectives, this paper continues and enhances the work that has been performed in [20]. The remainder of this paper is organized as follows. Section 2 outlines the overall methodology. Section 3 presents the test system configuration and parameters. In Section 4, the overall analysis, including the reliability analysis at the substation level and the reliability evaluation at the composite system level, is performed. Also, the results are presented and summarized. The scalability of the overall methodology performed in this paper is illustrated in Section 5. Some major considerations in software implementation for large power systems are discussed in Section 6. Finally, the conclusions are made in Section 7.

2. Methodology outline and objectives

The cyber-physical interdependencies exist in many aspects of power systems, including but not limited to supervisory control, protection, monitoring, metering, etc. This paper focuses on the aspect of protection since protection hidden failures are recognized as common causes of expanded outages and have significant impact on power system reliability [4–10].

In this paper, reliability evaluation is performed in a composite power system consisting of current-carrying components and protection systems. The Roy Billinton Test System (RBTS) [21] is used as the test system with extensions at load buses to include detailed configuration in terms of protection system elements.

The size of this system is small to permit reasonable time for extension of cyber part and development of interface matrices but the configuration of this system is sufficiently detailed to reflect the actual features of a practical system [22]. The methodology performed in this paper also applies for large systems. For large systems, in spite of more efforts needed in detailed analysis of cyber failure modes as well as effects on the physical side, the main procedures are identical to those performed in this paper. In short, the selected system is adequate to illustrate the methodology and extension to larger systems is more mechanical effort rather than illustrating the validity of the technique.

The overall analysis mainly consists of two stages: (1) reliability analysis of protection systems at the substation level and (2) reliability evaluation from the system-wide perspective.

2.1. Reliability analysis at the substation level

The failure modes of protection systems in terms of basic cyber elements and their relationships to transmission line tripping scenarios are analyzed in this stage. The CPIMs, which depict the interdependencies among the failures of physical components due to various cyber failure modes, are obtained at the end of this stage.

2.2. Reliability evaluation from the system-wide perspective

In this stage, a sequential Monte Carlo simulation is performed on the composite system to obtain system-wide reliability indices. The results of CPIMs obtained in the previous stage are directly utilized in this stage without the necessity of considering protection system configuration details. At the end of this stage, system-wide reliability indices, such as Loss of Load Probability (LOLP), Loss of Load Expectation (LOLE), Expected Energy Not Supplied (EENS), and Expected Frequency of Load Curtailment (EFLC), for each bus and for the overall system, can be obtained.

2.3. System-wide reliability indices

The following system-wide reliability indices [7,9,22] are defined and used in this paper.

2.3.1. Loss of load probability (LOLP)

$$\mathrm{LOLP} = \sum_{i=1}^{N_s} \frac{H_i t_i}{t_{\mathrm{total}}} \tag{1}$$

where,

N_s is total number of iterations simulated;

H_i equals 1 if load curtailment occurs in the ith iteration; otherwise it equals 0;

t_i is simulated time in the ith iteration, with the unit of year; and

t_{total} is total simulated time, with the unit of year.

2.3.2. Loss of load expectation (LOLE)

$$\mathrm{LOLE} = \mathrm{LOLP} \times 8760 \tag{2}$$

with the unit of hours/year.

2.3.3. Expected energy not supplied (EENS)

$$\mathrm{EENS} = \sum_{i=1}^{N_s} \frac{8760 R_i t_i}{t_{\mathrm{total}}} \tag{3}$$

with the unit of MWh/year,

where,

N_s is total number of iterations simulated;

R_i is load curtailment during the ith iteration, with the unit of MW;

t_i is simulated time in the ith iteration, with the unit of year; and

t_{total} is total simulated time, with the unit of year.

2.3.4. Expected frequency of load curtailment (EFLC)

$$\mathrm{EFLC} = \sum_{i=2}^{N_s} \frac{Z_i}{t_{\mathrm{total}}} \tag{4}$$

with the unit of (/year),

where,

N_s is total number of iterations simulated;

Z_i equals 1 if load curtailment does not happen in the $(i-1)$th iteration AND load curtailment happens at the ith iteration; otherwise it equals 0; and

t_{total} is total simulated time, with the unit of year.

3. Test system configuration

The Roy Billinton Test System (RBTS) [21] is used as the test system in this paper. The single line diagram of the RBTS is shown

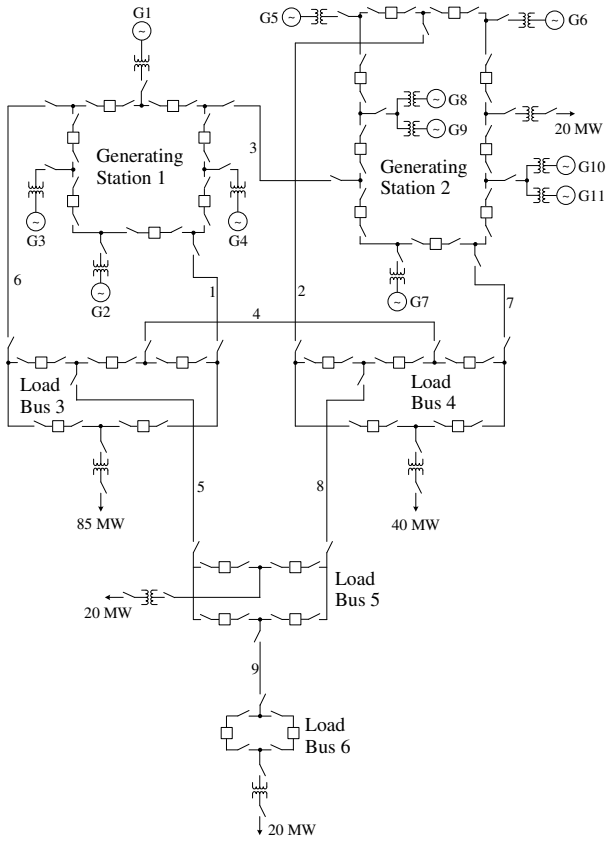

Fig. 1. Single line diagram of the RBTS.

Table 1
Bus data.

Bus no.	Name in Fig. 1	Peak load (p.u.)	Generation capacity (p.u.)
1	Generating station 1	0.00	1.10
2	Generating station 2	0.20	1.30
3	Load bus 3	0.85	0
4	Load bus 4	0.40	0
5	Load bus 5	0.20	0
6	Load bus 6	0.20	0

in Fig. 1. The bus, generation, load, and transmission line data are also provided in this section. In this paper, 100 MVA and 230 kV are used as the base values of power and voltage.

3.1. Bus, generation, and load data

The data for all the buses and generating units are obtained from [21] and are tabulated in Tables 1 and 2, respectively. A DC optimal power flow model is used in case of load curtailment. Therefore, only the real power data are considered.

Table 2
Generating unit data.

Unit no.	Bus	Rating (MW)	Failure rate (/year)	MRT (h)
1	1	40	6.0	45
2	1	40	6.0	45
3	1	10	4.0	45
4	1	20	5.0	45
5	2	5	2.0	45
6	2	5	2.0	45
7	2	40	3.0	60
8	2	20	2.4	55
9	2	20	2.4	55
10	2	20	2.4	55
11	2	20	2.4	55

Table 3
Transmission line physical parameters.

Line no.	Buses		Reactance X (p.u.)	Current rating (p.u.)
	From	To		
1	1	3	0.180	0.85
2	2	4	0.600	0.71
3	1	2	0.480	0.71
4	3	4	0.120	0.71
5	3	5	0.120	0.71
6	1	3	0.180	0.85
7	2	4	0.600	0.71
8	4	5	0.120	0.71
9	5	6	0.120	0.71

3.1.1. Generation variation

The generators are represented by reliability models with two states, up and down. The corresponding failure rate and Mean Repair Time (MRT) are obtained from [21] and are tabulated in Table 2.

3.1.2. Load variation

The annual peak load data for each bus are obtained from [21] and are shown in Table 1. The hourly load profile is created based on the information in Tables 1–3 of the IEEE Reliability Test System [23].

3.2. Transmission line data

The transmission line physical parameters and outage data are obtained from [21] and are tabulated in Tables 3 and 4, respectively.

A DC optimal power flow model with simplified line parameters is used in case of load curtailment. Therefore, the line resistance (R) as well as the charging susceptance (B) are not considered in the transmission line model and only the line reactance (X) is provided in Table 3. Furthermore, in the DC optimal power flow model, since the voltage magnitude at each bus is assumed to be 1.0 p.u., the current rating for each line shown in Table 3 is numerically equal to the power rating.

For the transmission line outage data, compared with [21], the transient outage (normally with duration of less than one minute) is not considered in this paper. Instead, a new term *switching time* is defined. The switching time for each transmission line, which is tabulated in Table 4, defines the time needed to switch a line back to service when this line is tripped due to a protection failure rather than resulting from a primary fault occurs at this line. The reciprocal of a switching time is called a *switching rate* and has been illustrated in [20].

Table 4
Transmission line outage data.

Line no.	Buses		Permanent outage rate (/year)	Outage duration (h)	Switching time (h)
	From	To			
1	1	3	1.5	10.0	4.0
2	2	4	5.0	10.0	4.0
3	1	2	4.0	10.0	4.0
4	3	4	1.0	10.0	4.0
5	3	5	1.0	10.0	4.0
6	1	3	1.5	10.0	4.0
7	2	4	5.0	10.0	4.0
8	4	5	1.0	10.0	4.0
9	5	6	1.0	10.0	4.0

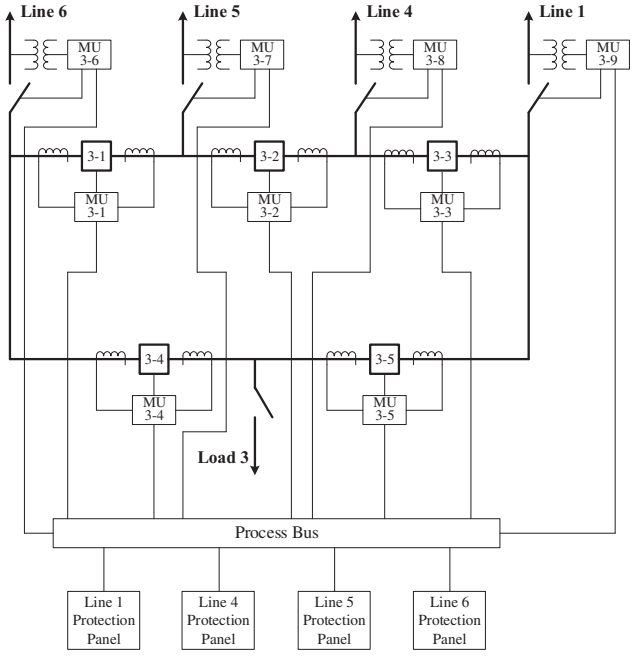

Fig. 2. The protection system for bus 3.

3.3. Protection system architecture and reliability data

For bus 6, since it is connected with only one transmission line (line 9), even if its own protection system fails, line 9 will always be de-energized by opening the breakers at bus 5 without isolating any other lines. Therefore, the protection system configuration at bus 6 is not considered and only buses 3, 4, and 5 in the RBTS are extended to include detailed protection system configurations, as shown in Figs. 2, 3 and 4 respectively.

The reliability data for Circuit Breakers (CBs), Merging Units (MUs), Process Buses (PBs), and Line Protection Panels are tabulated

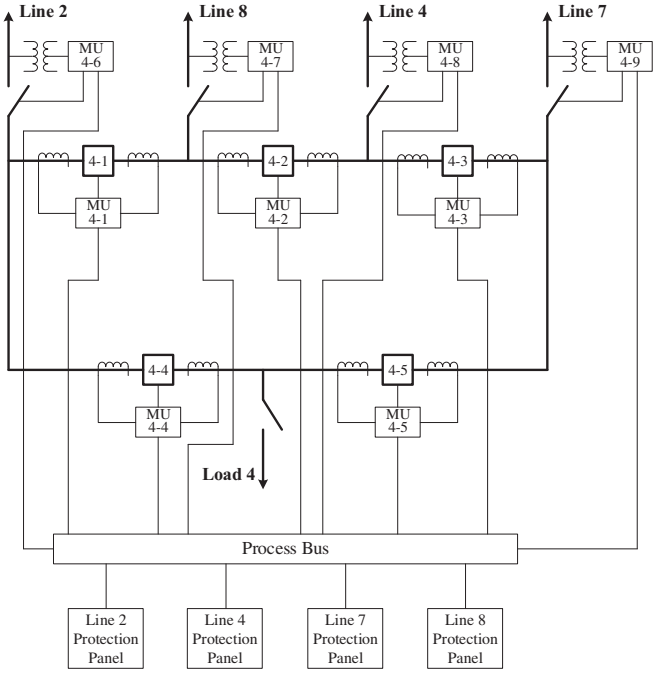

Fig. 3. The protection system for bus 4.

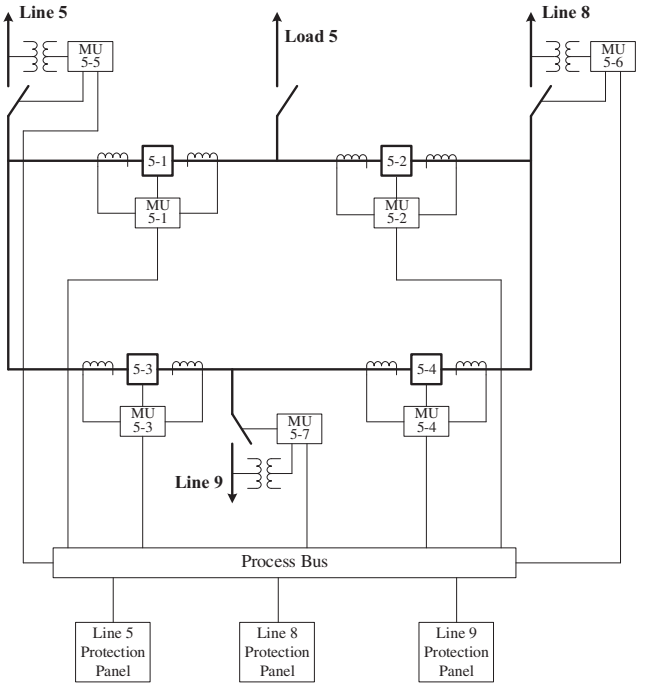

Fig. 4. The protection system for bus 5.

Fig. 5. State transition diagram of individual element.

in Table 5. We assume that a same type of elements at different substations are identical and thereby have the same reliability data.

According to engineering practice, the Mean Time to Failure (MTTF) varies for Circuit Breakers at different voltage levels, or serving different functions in the system [24]. For the study in this paper, a typical value of 100 years is chosen for the MTTF and a value of 8 h is used for the Mean Repair Time (MRT).

The reliability data for MUs, PBs, and Line Protection Panels are reasonably chosen based on the information from [14,25–27].

In this study, only two states, UP and DOWN, are considered for each protection system element (except the process bus) listed in Table 5. The state transition diagram is shown in Fig. 5. The failure and repair rates are denoted by λ and μ, respectively.

The exponential distribution is assumed for state residence times of each element, the probabilities of UP and DOWN can be calculated using Eqs. (5) and (6), respectively.

$$p_{\mathrm{UP}} = \frac{\mu}{\lambda + \mu} \tag{5}$$

$$p_{\mathrm{DOWN}} = \frac{\lambda}{\lambda + \mu} \tag{6}$$

Table 5
Reliability data for protection system elements.

Element name	MTTF (year)	Failure rate λ (/year)	MRT (h)	Repair rate μ (/year)
CB	100	0.01	8	1095
MU	50	0.02	8	1095
PB	100	0.01	8	1095
Line protection panel	50	0.02	8	1095

Fig. 6. State transition diagram of the process bus.

For the Process Bus (PB), an additional state representing DELAY is included as shown in Fig. 6. The probability of delay given that the PB is not in the DOWN state is denoted by p_d(=0.003). The illustration of this reliability model as well as the discussion regarding delay issues in substation communication networks have been presented in [20].

Therefore, for the Process Bus,

$$p_{\text{UP.PB}} = \frac{\mu}{\lambda+\mu}(1-p_d) \tag{7}$$

$$p_{\text{DELAY.PB}} = \frac{\mu}{\lambda+\mu}p_d \tag{8}$$

$$p_{\text{DOWN.PB}} = \frac{\lambda}{\lambda+\mu} \tag{9}$$

In reality, the process bus is a network consisting of basic elements that are connected with each other in various topologies and thus more sophisticated technical details are involved [26,28–31]. The consideration of these technical details in composite system reliability evaluation is beyond the scope of this paper and will be developed in our future work.

The assumptions regarding other protection elements such as Current Transformers (CTs)/Potential Transformers (PTs), cable links, etc. and protection issues such as backup tripping follow those stated in [20]. The CTs, PTs, and cable links are assumed not to fail. In addition, based on the features of this particular test system, several more assumptions are made:

a. The failure of an MU that is connected to a PT will result in the failure of acquired voltage information and thus will disable the primary protection of this line. As a result, multiple breakers associated with the primary protection will fail to trip and backup protections will be triggered. For example, in the bus 3 protection system (shown in Fig. 2), if a primary fault happens at Line 6 but MU 3-6 fails, then the Line 6 Protection Panel will fail to issue trip signals to both breakers 3-1 and 3-4. As a result, backup protection zones will be triggered and breakers 3-2 and 3-5 will trip to isolate Line 6.
b. Since this paper focuses on transmission system reliability evaluation and the details of a load branch can be extended in the distribution system. Primary faults that occur at load branches are not considered in this paper. However, the isolation of a load branch resulting from undesired trips due to primary faults that occur at adjacent transmission lines will be considered.

4. Reliability analysis

The overall analysis mainly consists of two stages: the reliability analysis of protection systems at the substation level and the reliability evaluation from the system-wide perspective. The CPIM, which bridges the two stages, is a critical idea of this methodology. It decouples the analysis of protection systems from the evaluation of the composite system and makes the overall analysis more tractable.

4.1. Substation level reliability analysis

The substation level reliability analysis follows the procedures described in [20] with the objective of obtaining CPIMs.

This paper improves the CPIM that was described in [20] by eliminating the off-diagonal zeros to make it more compact. In this paper, each row in a CPIM represents a physical component (transmission line). Each column provides the probability of a consequent event given that a primary fault occurred on this physical component. Therefore, the probabilities in each row sum up to 1. If the protection system is perfectly reliable, then the first column would have probabilities 1 and other columns zero.

In addition, another matrix, Consequent Event Matrix (CEM), is developed in accordance with a CPIM. A CEM provides detailed information about consequent events in which some lines go out of service while some are not affected. In a CEM, each event is coded as a 12-digit binary number, of which the left 9 digits correspond to the 9 transmission lines and the last 3 digits correspond to load branches 3, 4, and 5, respectively. A "1" digit indicates the corresponding component is going out of service whereas a "0" means this component is not affected. For example, an entry "100001100110" denotes a consequent event in which line 1, line 6, line 7, load branch 3, and load branch 4 are going out of service. A complete row of a CEM summarizes all possible consequent events when a primary fault occurs at this transmission line.

To illustrate how the malfunctions of cyber elements affect transmission line tripping behaviors, the detailed analysis for the consequent events resulting from cyber element failures at substation (bus) 3 following a primary fault occurs at line 1 is shown below as an example. The analysis for the primary faults at other lines can be performed similarly. In the analysis, the failure modes of individual cyber elements are assumed independent since they are located in different units in a substation. Therefore, the probability of a consequent event can be obtained by multiplying the probabilities of individual element states in this event.

Suppose a primary fault occurs at line 1, all possible consequent events can be categorized as follows.

(1) All protection elements operate as intended.

If all protection elements operate as intended, then only line 1 will be isolated. The action of line 1 tripping associated with these elements at substation 3: MU 3-9, CB 3-3, MU 3-3, CB 3-5, MU 3-5, Process Bus, and Line 1 Protection Panel. Multiply the UP probabilities of all these elements, the corresponding probability of this consequent event can be obtained, which is 0.996899850569.

(2) The Process Bus (PB) fails.

If the PB fails, then the entire substation will be affected by this fault. All lines connected to this substation will be isolated by tripping the breakers at remote substations. The corresponding probability of this consequent event can be calculated using Eq. (9). This is an extreme case therefore the probability is very low. However, once this event happens, the impact is tremendous.

(3) One or both of MU 3-3, CB 3-3 fail(s), while all other associated elements operate as intended.

In this case, CB 3-3 fails to trip while CB 3-5 trips as intended. The fault will be cleared by opening CB 3-2 and CB 3-5. As a result, Lines 1 and 4 will be isolated.

(4) One or both of MU 3-5, CB 3-5 fail(s), while all other associated elements operate as intended.

In this case, CB 3-5 fails to trip while CB 3-3 trips as intended. The fault will be cleared by opening CB 3-3 and CB 3-4. As a result, Line 1 and load branch 3 will be isolated.

(5) The Process Bus (PB) does not fail, but both CB 3-3 and CB 3-5 fail to trip due to various combinations of element states, such as Line 1 Protection Panel fails or the PB is in a DELAY state.

In this case, the fault will be cleared by opening CB 3-2 and CB 3-4. As a result, Line 1, Line 4, and load branch 3 will be isolated.

The results of all the 5 cases above are summarized in the first row of Table 6 and Table 7. It should be noted that these consequent events are the results from cyber element failures. If the all

Table 6
The cyber-physical interface matrix for bus 3.

Fault location	Probabilities				
Line 1	0.996899850569	0.000009132337	0.000027312491	0.000027312491	0.003036392112
Line 4	0.996899850569	0.000009132337	0.000027312491	0.000027312491	0.003036392112
Line 5	0.996899850569	0.000009132337	0.000027312491	0.000027312491	0.003036392112
Line 6	0.996899850569	0.000009132337	0.000027312491	0.000027312491	0.003036392112

Table 7
The consequent event matrix for bus 3.

Fault location	Events				
Line 1	100000000000	100111000000	100100000000	100000000100	100100000100
Line 4	000100000000	100111000000	000110000000	100100000000	100110000000
Line 5	000010000000	100111000000	000011000000	000110000000	000111000000
Line 6	000001000000	100111000000	000001000100	000011000000	000011000100

Table 8
The cyber-physical interface matrix for bus 4.

Fault location	Probabilities				
Line 2	0.996899850569	0.000009132337	0.000027312491	0.000027312491	0.003036392112
Line 4	0.996899850569	0.000009132337	0.000027312491	0.000027312491	0.003036392112
Line 7	0.996899850569	0.000009132337	0.000027312491	0.000027312491	0.003036392112
Line 8	0.996899850569	0.000009132337	0.000027312491	0.000027312491	0.003036392112

associated cyber elements are perfectly reliable, then the first case would have probability one while all other cases zero.

Following similar procedures performed above, the complete Cyber-Physical Interface Matrices (CPIMs) and Consequent Event Matrices (CEMs) for buses 3, 4, and 5 are obtained and are shown from Tables 6–11.

4.2. System-wide reliability evaluation

The next event sequential Monte Carlo simulation [32] forms the main framework for the reliability evaluation in this stage. The detailed steps, including illustrations on how to utilize the results of a CPIM in the composite system reliability evaluation [20], are summarized as follows.

a. Initialize.
b. *Determine a primary event*: Find the minimum time to the next event, update the corresponding element's state, and update the total time.
c. *Determine consequent events*: If the state change in step b indicates a primary fault occurring at a transmission line, then use CPIMs and CEMs to determine the consequent events and update elements' states accordingly. If a CPIM row corresponding to this transmission line has n consequent events, the probabilities of these events $(p_1, p_2, \ldots, p_n)$ sum up to 1. Draw a random number ranging from 0 to 1. The value of this random number determines which consequent event is going to happen. It should be noted that a transmission line connects two substations. Therefore, two random numbers should be drawn independently to determine the consequent event at each substation.
d. *Effects of switching and repair*: For elements whose states have been changed in step b or in step c, draw new random numbers to determine the time of their next transitions. Appropriate transition rates should be used according to situations.
e. *Evaluate system state*: Perform the network power flow analysis to assess system operation states. Update reliability indices.
f. Repeat steps b–e until convergence is achieved.

In step e, the following DC power flow linear programming model [33–35] is used with the objective of minimizing total load curtailment.Objective: $y = \mathrm{Min}\sum_{i=1}^{N_b} C_i$

subject to:

$$\begin{aligned} \hat{B}\theta + G + C &= L \\ G &\le G^{\max} \\ C &\le L \\ DA\theta &\le F^{\max} \\ -DA\theta &\le F^{\max} \\ G, C &\ge 0 \\ \theta_1 &= 0 \\ \theta_{2\ldots N_b} &\text{ unrestricted} \end{aligned} \tag{10}$$

where,
N_b is number of buses;
C is an $N_b \times 1$ vector of bus load curtailments;
C_i is load curtailment at bus i;
$\hat{B}$ is an $N_b \times N_b$ augmented node susceptance matrix;
G is an $N_b \times 1$ vector of bus actual generating power;
$G^{\max}$ is an $N_b \times 1$ vector of bus maximum generating availability;
L is an $N_b \times 1$ vector of bus loads;

Table 9
The consequent event matrix for bus 4.

Fault location	Events				
Line 2	010000000000	010100110000	010000000010	010000010000	010000010010
Line 4	000100000000	010100110000	000100010000	000100100000	000100110000
Line 7	000000100000	010100110000	000100100000	000000100010	000100100010
Line 8	000000010000	010100110000	010000010000	000100010000	010100010000

Table 10
The cyber-physical interface matrix for bus 5.

Fault location	Probabilities				
Line 5	0.996899850569	0.000009132337	0.000027312491	0.000027312491	0.003036392112
Line 8	0.996899850569	0.000009132337	0.000027312491	0.000027312491	0.003036392112
Line 9	0.996899850569	0.000009132337	0.000027312491	0.000027312491	0.003036392112

Table 11
The consequent event matrix for bus 5.

Fault location	Events				
Line 5	000010000000	000010011000	000010001000	000010000001	000010001001
Line 8	000000010000	000010011000	000000010001	000000011000	000000011001
Line 9	000000001000	000010011000	000000011000	000010001000	000010011000

Table 12
Reliability indices for buses.

	LOLP	LOLE (h/year)	EENS (MWh/year)	EFLC (/year)
Bus 1	0	0	0	0
Bus 2	0.00015926	1.395	2.655	0.260
Bus 3	0.00017063	1.495	8.597	0.300
Bus 4	0.00019288	1.690	10.095	0.315
Bus 5	0.00016786	1.470	3.729	0.275
Bus 6	0.00124176	10.878	116.104	1.305
Overall system	0.00128584	11.264	141.180	1.395

D is an $N_t \times N_t$ diagonal matrix of transmission line susceptances, with N_t the number of transmission lines;

A is an $N_t \times N_b$ line-bus incidence matrix;

θ is an $N_b \times 1$ vector of bus voltage angles; and

F^{max} is an $N_t \times 1$ vector of transmission line power flow capacities.

In Eq. (10), the variables are vectors θ, G, and C. Thus, the total number of variables is $3N_b$. This problem can be solved by using the *linprog* function provided in MATLAB software.

The convergence is measured by the coefficient of variation of a chosen index, as defined in [22]. A simulation with 200 simulated years is performed and the coefficient of variation for the system EENS drops below 5%.

4.3. Results and discussions

The simulation results of LOLP, LOLE, EENS, and EFLC for each bus and for the overall system are tabulated in Table 12. The simulated transmission line failure rates due to primary faults and protection system malfunctions are tabulated in Table 13. In Table 13, for line 3, the simulated line failure rate due to protection system malfunctions equals 0. This is because line 3 links bus 1 to bus 2 and protection malfunctions are not considered for either of the two buses.

Table 13
Simulated transmission line failure rates.

Line no.	Failure rate resulting from primary faults (/year)	Failure rate resulting from protection malfunctions (/year)
1	1.455	0.010
2	4.850	0.005
3	3.870	0
4	1.030	0.075
5	0.925	0.010
6	1.570	0.010
7	5.100	0.005
8	1.080	0.010
9	1.030	0.010

To make a comparison, the situation in which protection systems are assumed perfectly reliable is also simulated with results tabulated in Table 14. The comparison is also displayed in Fig. 7.

The results in Tables 13 and 14 show that protection system malfunctions have significant impact on energy unavailability even though they do not have much impact on individual line failure rates. Compared with not considering protection malfunctions, the percentage increment of the EENS for individual buses can be quite significant.

The effects of protection system malfunctions on EENS are noticeable for buses 3, 4, and 5, with increments of 204.00%, 417.69%, and 73.85%, respectively. These three buses are also the ones in which we have modeled and considered protection system malfunctions. This further points to the impact of protection malfunctions on energy unavailability.

4.4. The effects of switching time

A value of 4.0 h is assumed as the switching time for all transmission lines and this value has been used in all previous analysis.

In engineering practice, a switching process may be accelerated with the aid of smart grid technologies, or may be prolonged due to other factors. The quantitative relationship between switching time and system EENS are studied and the results are shown in Table 15. In each case, same value of switching time is assumed for all transmission lines and the system EENS is compared with the case in which the switching time is 4.0 h. This relationship is also displayed in Fig. 8.

The information in Table 15 and Fig. 8 indicates a close relationship between the line switching time and the system EENS. The value of system EENS increases considerably with prolonged switching time. This also signifies the importance of using advanced technologies with which the process of fault location and cyber failure identification would be accelerated so that healthy lines can be switched back to service more promptly.

Table 14
EENS comparison.

	EENS (MWh/year)		Δ (%)
	If protection systems are perfectly reliable	Considering protection malfunctions	
Bus 1	0	0	N/A
Bus 2	1.862	2.655	42.59
Bus 3	2.828	8.597	204.00
Bus 4	1.950	10.095	417.69
Bus 5	2.145	3.729	73.85
Bus 6	103.947	116.104	11.70
Overall system	112.732	141.180	25.24

For each row, Δ is defined as the percentage increment of the EENS from not considering to considering protection malfunctions.

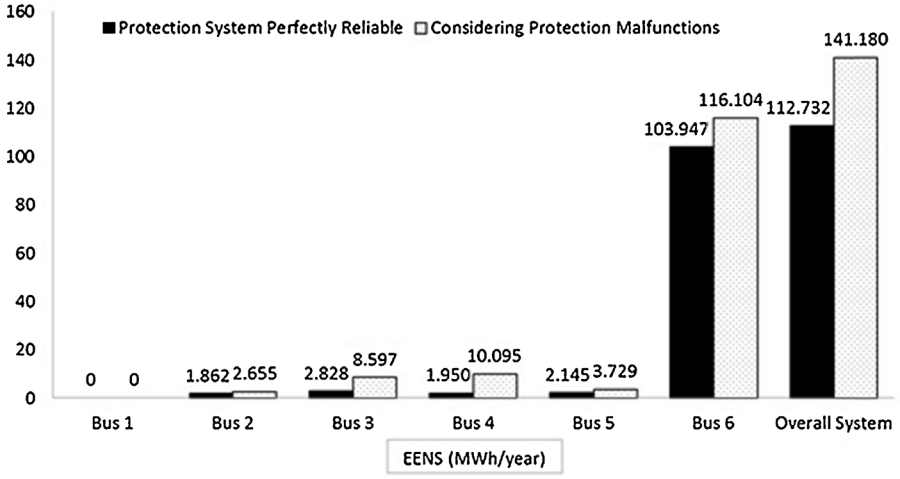

Fig. 7. EENS comparison at each bus.

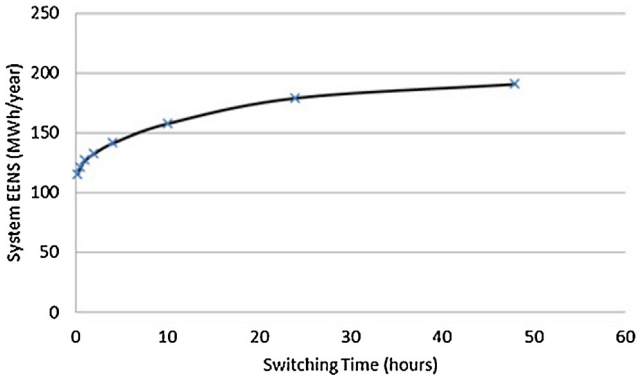

Fig. 8. Relationship between switching time and system EENS.

5. The scalability of the overall methodology

As shown in Section 4, the overall methodology consists of two stages:

1. Reliability analysis at the substation level (i.e., the work performed in Section 4.1).
2. System-wide reliability evaluation (i.e., the work performed in Section 4.2).

In the first stage, the detailed analysis depends on the actual protection architecture of a substation. The analysis may seem to be tedious for a substation with complex architecture. However, the analysis in this stage can be performed locally at each substation and the computations can be performed offline. The increased workload for more complex substations does not change the framework of the overall methodology. It should be noted that although in this stage, the analysis is needed for each individual substation, with more experience in the analysis at substation level, it may be possible to generate classifications into types of substations and thus expedite the process.

Once the CPIMs and CEMs are established in the first stage, they can be permanently stored and can be directly plugged into the reliability evaluation in the second stage. The Monte-Carlo simulation performed in the second stage is generic and applicable for large power systems.The CPIM decouples the first stage of analysis from the second stage and makes the overall analysis more tractable.

Table 15
Effect of switching time on system EENS.

Switching time (h)	System EENS (MWh/year)	Percentage increment/decrement compared with the value of 141.180 MWh/year in Table 14
0.2	115.089	−18.48
0.5	120.941	−14.34
1	126.945	−10.08
2	132.675	−6.02
4	141.180	0
10	157.615	+11.64
24	178.986	+26.78
48	190.628	+35.02

6. Considerations in software implementation for large power systems

The methodology proposed in this paper establishes a framework for power system reliability evaluation considering cyber-malfunctions in substations. Some implementation considerations are important to its application for large power systems. This section discusses two major considerations, the CPU time for Monte Carlo simulation and the storage of matrices. At the outset we can say that some implementation issues will need to be worked out but there do not appear to be any insurmountable barriers.

6.1. CPU time for Monte Carlo simulation

The convergence in a Monte Carlo simulation is measured by the coefficient of variation of a chosen index. In this paper, simulation is performed for 200 years and the coefficient of variation for the system EENS drops below 5%. The simulation for this paper is performed in MATLAB running on a computer with a 3.10 GHz processor and the running time for a simulation is approximately 8 min. It should be noted that this software implementation of the simulation is only research grade to illustrate the concept and is therefore not the most efficient as far as the running time is concerned. The running time is largely consumed by the *linprog* function in MATLAB for DC power flow based linear programming to evaluate system operation states. In the development of a commercial grade program, the running time can be drastically reduced by several means as described below.

1. The linear programming incorporating DC power flow can be performed less frequently with the use of heuristic algorithms for screening, thus reducing the CPU time.

2. Simulation can be custom coded in more efficient programming languages. Custom programs are generally more efficient than generic ones coded in MATLAB.
3. Much more efficient methods such as interior point methods can be used for linear programming.
4. Monte Carlo simulation is readily amenable to parallel and distributed processing environments [36,37] to reduce the CPU time.

It is important to mention that Monte Carlo simulation has already been successfully used for large composite power systems but without considering the cyber-malfunctions. The contribution of this paper is to develop a methodology to include cyber induced dependent failures in such Monte Carlo programs. The cyber induced dependent failures can be included in Monte Carlo simulation by using CPIMs. This does not significantly alter the number of times linear programming is called for and thus does not alter the CPU time much.

6.2. Storage of matrices

For a given power system, let m be the total number of rows in all CPIMs (or CEMs), n be the number of columns in a CPIM (or a CEM).

The value of m depends on the number of transmission lines. The number of transmission lines in an actual power system is typically 1.2–2 times of the number of buses. Each transmission line contributes a row in two CPIMs (or CEMs) corresponding to both of the two buses it connects to. Consider a power system with 1000 buses (substations), which is a typical size of an actual transmission grid, it is reasonable to estimate the number of transmission lines as 2000 and thus the value of m is estimated to be 4000.

The value of n is determined by the row with maximum number of consequent events, which depends on the transmission line having maximum number of adjacent lines. Assuming a transmission line has maximum 10 adjacent lines, thus the maximum possible value of n is 2^{10}, which is 1024. Of course, it is possible that a few transmission lines may have more than 10 adjacent lines. For such lines, only the 1024 most likely consequent events are considered since the remaining consequent events have negligible probabilities. Thus, it is reasonable to estimate n as 1024.

Each entry in a CPIM can be stored as a 64-bit double-precision floating-point number. Therefore, the total storage space needed for all CPIMs is $8{\cdot}m{\cdot}n$ Bytes, which equals 31.25 MB (32,768,000 Bytes).

Each entry in a CEM is a binary number corresponding to a consequent event. For a system with 2000 transmission lines, 2000 bits are needed to represent such an event. Thus, each entry uses 250 Bytes (2000 bits) and the total storage space needed for all CEMs is $250{\cdot}m{\cdot}n$ Bytes, which equals 976.5625 MB (1,024,000,000 Bytes).

Therefore, the total space needed to store all CPIMs and CEMs is estimated to be 1007.8125 MB, which is approximately 0.9842 GB. It is feasible to claim such space on hard drive or Random Access Memory (RAM).

7. Conclusions

In this paper, a systematic reliability evaluation methodology is implemented in a composite power system consisting of current-carrying components and protection systems with modern architecture. The quantitative relationship between switching time and system EENS is also studied. The results clearly indicate the impact of protection failures on system-wide reliability indices and also signify the importance of accelerating line switching process.

The methodology implemented in this paper is scalable and provides an option for the reliability evaluation of large cyber-physical power systems. For such systems, in spite of more efforts needed in detailed analysis, the main procedures remain similar to those performed in this paper.

Acknowledgments

This paper was made possible by the Power Systems Engineering Research Center (PSERC) under the grant “Reliability Assessment and Modeling of Cyber Enabled Power Systems with Renewable Sources and Energy Storage (T-53)” and by NPRP grant # NPRP 7-106-2-053 from the Qatar National Research Fund (a member of Qatar Foundation). The statements made herein are solely the responsibility of the authors.

References

[1] R. Billinton, Power system reliability evaluation, Gordon and Breach, New York, 1970.
[2] R. Billinton, R.N. Allan, Reliability assessment of large electric power systems, Kluwer, Boston, 1988.
[3] R. Billinton, W. Li, Reliability assessment of electric power systems using Monte Carlo methods, Plenum Press, New York, 1994.
[4] A.G. Phadke, J.S. Thorp, Expose hidden failures to prevent cascading outages, IEEE Comput. Appl. Power 9 (3) (1996) 20–23.
[5] D.C. Elizondo, J. De La Ree, A.G. Phadke, S. Horowitz, Hidden failures in protection systems and their impact on wide-area disturbances, Proceedings of IEEE power engineering society winter meeting, January/February 2001, vol. 2, pp. 710–714.
[6] F. Yang, A.P.S. Meliopoulos, G.J. Cokkinides, Q.B. Dam, Effects of protection system hidden failures on bulk power system reliability, Proceedings of the 38th IEEE North American power symposium, September 2006, pp. 517–523.
[7] X. Yu, C. Singh, A practical approach for integrated power system vulnerability analysis with protection failures, IEEE Trans. Power Syst. 19 (November (4)) (2004) 1811–1820.
[8] R. Billinton, J. Tatla, Composite generation and transmission system adequacy evaluation including protection system failure modes, IEEE Trans. Power App. Syst. PAS-102 (June (6)) (1983) 1823–1830.
[9] M.C. Bozchalui, M. Sanaye-Pasand, M. Fotuhi-Firuzabad, Composite system reliability evaluation incorporating protection system failures, Proceedings of the 2005 IEEE Canadian conference on electrical and computer engineering, May 2005, pp. 486–489.
[10] K. Jiang, C. Singh, New models and concepts for power system reliability evaluation including protection system failures, IEEE Trans. Power Syst. 26 (November (4)) (2011) 1845–1855.
[11] S.H. Horowitz, A.G. Phadke, Power system relaying, 3rd ed., John Wiley & Sons Ltd, Chichester, West Sussex, UK, 2008.
[12] J.L. Blackburn, T.J. Domin, Protective relaying: principles and applications, 3rd ed., CRC, Boca Raton, FL, USA, 2007.
[13] P.M. Anderson, Power System Protection—Part VI: reliability of protective systems, McGraw-Hill/IEEE Press, New York, 1999.
[14] B. Kasztenny, J. Whatley, E.A. Udren, J. Burger, D. Finney, M. Adamiak, Unanswered questions about IEC 61850—what needs to happen to realize the vision? Presented at the 32nd annual western protective relay conference, Spokane, WA, USA, October 2005.
[15] T. Skeie, S. Johannessen, C. Brunner, Ethernet in substation automation, IEEE Control Syst. Mag. 22 (June (3)) (2002) 43–51.
[16] T.S. Sidhu, P.K. Gangadharan, Control and automation of power system substation using IEC 61850 communication, Proceedings of the 2005 IEEE conference on control applications, August 2005, pp. 1331–1336.
[17] J.D. McDonald, Electric power substations engineering, 3rd ed., CRC, Boca Raton, FL, USA, 2012.
[18] B. Falahati, Y. Fu, L. Wu, Reliability assessment of smart grid considering direct cyber-power interdependencies, IEEE Trans. Smart Grid 3 (September (3)) (2012) 1515–1524.
[19] B. Falahati, Y. Fu, Reliability assessment of smart grids considering indirect cyber-power interdependencies, IEEE Trans. Smart Grid 5 (July (4)) (2014) 1677–1685.
[20] H. Lei, C. Singh, A. Sprintson, Reliability modeling and analysis of IEC 61850 based substation protection systems, IEEE Trans. Smart Grid 5 (September (5)) (2014) 2194–2202.
[21] R. Billinton, S. Kumar, N. Chowdhury, K. Chu, K. Debnath, L. Goel, E. Khan, P. Kos, G. Nourbakhsh, J. Oteng-Adjei, A reliability test system for educational purposes-basic data, IEEE Trans. Power Syst. 4 (August (3)) (1989) 1238–1244.
[22] A. Sankarakrishnan, R. Billinton, Sequential Monte Carlo simulation for composite power system reliability analysis with time varying loads, IEEE Trans. Power Syst. 10 (August (3)) (1995) 1540–1545.
[23] IEEE Committee Report, IEEE reliability test system, IEEE Trans. Power App. and Syst. PAS-98 (November/December (6)) (1979) 2047–2054.

[24] T.M. Lindquist, L. Bertling, R. Eriksson, Circuit breaker failure data and reliability modeling, IET Gener. Transm. Distrib. 2 (November (6)) (2008) 813–820.
[25] M.G. Kanabar, T.S. Sidhu, Reliability and availability analysis of IEC 61850 based substation communication architectures, Presented at the IEEE power & energy society general meeting, Calgary, AB, Canada, 2009.
[26] V. Skendzic, I. Ender, G. Zweigle, IEC 61850-9-2 process bus and its impact on power system protection and control reliability, Schweitzer Engineering Laboratories, Inc., Pullman, WA, USA, Technical Report, 2007.
[27] K.P. Brand, V. Lohmann, W. Wimmer, Substation automation handbook, utility automation consulting Lohmann, Bremgarten, Switzerland, 2003.
[28] M.G. Kanabar, T.S. Sidhu, Performance of IEC 61850-9-2 process bus and corrective measure for digital relaying, IEEE Trans. Power Del. 26 (April (2)) (2011) 725–735.
[29] L. Andersson, K.-P. Brand, C. Brunner, W. Wimmer, Reliability investigations for SA communication architectures based on IEC 61850, Presented at the IEEE PowerTech, St. Petersburg, Russia, June 2005.
[30] A. Apostolov, B. Vandiver, IEC 61850 process bus—principles, applications and benefits, Proceedings of the 63rd annual conference on protective relay engineers, 2010, pp. 1–6.
[31] P. Ferrari, A. Flammini, S. Rinaldi, G. Prytz, Mixing real time Ethernet traffic on the IEC 61850 process bus, Proceedings of the 9th IEEE international workshop on factory communication systems (WFCS), Lemgo, Germany, May 21–24, 2012, pp. 153–156.
[32] C. Singh, J. Mitra, Monte Carlo simulation for reliability analysis of emergency and standby power systems, Proceedings of the 30th IEEE industry applications society conference, Orlando, FL, October 1995, pp. 2290–2295.
[33] C. Singh, J. Mitra, Composite system reliability evaluation using state space pruning, IEEE Trans. Power Syst. 12 (February (1)) (1997) 471–479.
[34] EPRI, Composite system reliability evaluation methods, Final report on research project 2473-10, EPRI EL-5178, June 1987.
[35] J. Mitra, C. Singh, Incorporating the DC load flow model in the decomposition-simulation method of multi-area reliability evaluation, IEEE Trans. Power Syst. 11 (August (3)) (1996) 1245–1254.
[36] N. Gubbala, C. Singh, Models and considerations for parallel implementation of Monte Carlo simulation methods for power system reliability evaluation, IEEE Trans. Power Syst. 10 (May (2)) (1995) 779–787.
[37] C.L.T. Borges, D.M. Falcão, Carlos João, O. Mello, A.C.G. Melo, Composite reliability evaluation by sequential Monte Carlo simulation on parallel and distributed processing environments, IEEE Trans. Power Syst. 16 (May (2)) (2001) 203–209.